Int. J. Heat Mass Transfer. Vol. 36, No. 18, pp. 4307–4316, 1993
Printed in Great Britain

0017–9310/93 $6.00+0.00

Mixing between a sharp-edged rectangular jet and a transverse cross flow

A. J. HUMBER, E. W. GRANDMAISON and A. POLLARD†
Department of Chemical Engineering and † Department of Mechanical Engineering, Queen's University, Kingston, Ontario K7L 3N6, Canada

(*Received* 30 *July* 1992 *and in final form* 17 *June* 1993)

Abstract—The scalar mixing field of a turbulent rectangular jet issuing from a sharp-edged orifice with an aspect ratio of 10 into a cross stream flow in a square duct is investigated using marker nephelometry. Jet-to-cross stream velocity ratios of 2.0 and 3.4 are examined in this work. Results include contour plots and transverse profiles of the mean and concentration fluctuation intensity and jet trajectory paths and half concentration lengths expressed as a function of downstream position along the jet trajectory.

BACKGROUND

THE MIXING field arising between a jet and a transverse cross flow has received considerable attention in the engineering literature. This research arises from a wide interest in this flow geometry for applications including turbine heat transfer, VTOL applications, pollutant dispersion and chemical mixing problems. Of particular interest in this regard is the case of a round jet with an average exit velocity U_j mixing with a cross stream of uniform velocity U_0. The resulting flow patterns including descriptions of the jet trajectory and complex three-dimensional vortex structure have been investigated for the single jet [1–19] and multiple jets [20–27] in cross flows. The scalar mixing field arising from the round jet in a cross flow also has been examined, [3, 5, 10, 28–30]. Mathematical modelling of this complex flow system has been based on integral methods [31–33] and numerical methods [34–38].

In the present work, interest was focused on the scalar mixing field of a rectangular jet in a transverse flow for applications in secondary and tertiary ducts in industrial boiler/furnace systems. The jet trajectory, Fig. 1, can be described in terms of Cartesian coordinates (X, Y, Z) or an orthogonal system (ξ, η, ζ) with the ξ-axis located on the jet trajectory. In the industrial applications of interest, air is induced into a furnace chamber under negative pressure (on the order of 0.25 kPa) resulting in velocity ratios typically in the range of $2 < U_j/U_0 < 4$. The jet nozzle was a sharp edged rectangular orifice with an aspect ratio of 10—this geometry was chosen for its ease of construction and for comparison with some properties already published for the free jet behaviour of this jet geometry [39–41].

The flow field arising from a sharp-edged rectangular jet has been extensively studied and much of the literature in this field has been described in refs [41, 42]. The essential features of this flow include: (i) a saddle-back profile of the mean velocity and nozzle scalar fluid in the plane or major axis of the rectangular jet; (ii) transverse jet scales (as measured by the half velocity or concentration points on the major and minor axes) that are initially smaller along the minor axis but tend to a similar magnitude farther downstream; and (iii) high entrainment rates as indicated by the centreline mean concentration decay.

The scalar mixing field of a round jet injected into cross flow streams has been examined using gaseous tracer species [3, 10]; a weak temperature field introduced by the jet flow [5, 28, 30]; and an oil smoke tracer [29]. These studies have served to identify suitable empirical expressions based on dimensional reasoning for the jet trajectory in terms of the velocity ratio, U_j/U_0, and downstream position from the nozzle source, X (Rathgeber and Becker [29] also examined the effect of jet/pipe dimensions for a jet injected in a pipe flow). The jet penetration based on the scalar concentration field has also been found to be less than the trajectory found from velocity data [5]. Previous work on the scalar field has also indicated

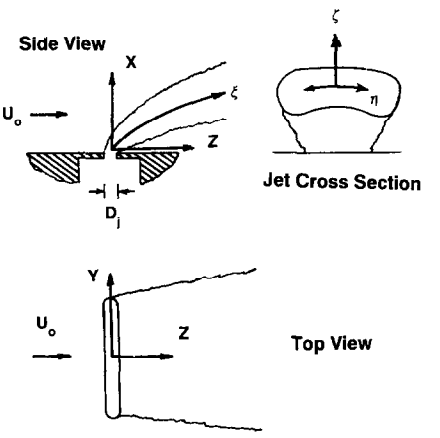

FIG. 1. Schematic diagram of the rectangular jet in a cross flow stream.

NOMENCLATURE

- b transverse concentration half width, point where $\bar{\Gamma} = 1/2\ \bar{\Gamma}_{max}$
- D_j jet dimension on the minor jet axis
- D_e equivalent diameter of a round jet with the same cross sectional area
- f_1, f_2 function of, in equations (1) and (2)
- L_j jet dimension on the major axis
- R velocity ratio, U_j/U_0
- U_j jet velocity
- U_0 cross stream velocity
- X Cartesian coordinate along the jet axis
- Y Cartesian coordinate transverse to X-plane
- Z Cartesian coordinate transverse to X-plane.

Greek symbols

- γ' concentration fluctuation, $\bar{\Gamma} - \Gamma$
- Γ total concentration
- ζ orthogonal coordinate transverse to ξ-plane
- η orthogonal coordinate transverse to ξ-plane
- ξ orthogonal coordinate along jet trajectory
- ρ_j density of jet fluid
- ρ_0 density of cross stream fluid.

Subscripts

- x property in X-direction
- y property in Y-direction
- 1/2 reference to a half concentration point defined by $\bar{\Gamma}/\bar{\Gamma}_{max} = 0.5$ contours.

Superscripts

- $\bar{}$ time average value
- $'$ r.m.s. value.

that at velocity ratios, U_j/U_0, greater than 4, a maximum in the concentration field occurs off the jet trajectory in the counter rotating vortex [5, 29]. Most of this work has involved a jet originating from a boundary wall (either a wind tunnel, duct or pipe) and it is possible that such a boundary alters the evolution of the entrainment and mixing process; photographic evidence of this phenomenon was reported for example by Keffer and Baines [1].

Weston and Thames [43] have studied some features of the flow arising from a rectangular jet with an aspect ratio of 4 injected into a cross flow. Both orientations of the jet relative to the free stream velocity (major axis either normal or parallel to the flow) were investigated in this work. Krothapalli *et al.* [44] have recently examined the separated flow region upstream of rectangular jets in a cross flow. They found that the normalized separation distance reached a maximum near $U_j/U_0 \approx 5$ and subsequently decreased in a linear manner at larger velocity ratios.

The dimensionless parameters relevant for the jet in a cross flow have been described in previous work [1, 2, 29]. The most important factor is the momentum ratio of the jet fluid to the cross stream flow. In the present work a rectangular jet in a cross flow was examined in a wind tunnel working section. Jet dimensions and velocity ratios were chosen to minimize the effect of the jet-to-duct dimension (this ratio was 0.027, close to the minimum value of this parameter examined by Rathgeber and Becker [29]). Hence, the parameters describing the jet trajectory can be expressed in the form described by Pratte and Baines [2],

$$X/RD_j = f_1(Z/RD_j) \quad \text{or} \quad X/RD_j = f_2(\xi/RD_j). \quad (1)$$

The rectangular jet diameter can also be expressed in terms of the diameter of round jet with the same cross sectional area ($D_e = 21.2$ mm $= 3.34\ D_j$ in this case) however, the correlations presented in this work are not sensitive to this refinement. The majority of the results presented in this work are for the near field region where the narrow jet dimension is deemed to be the most relevant scaling parameter. It can also be noted that the dependent variables could also be expressed in the form of X/R^2D_j as suggested by Keffer and Baines [1] but the forms of equation (1) are adopted in this work for later comparison with measurements of Pratte and Baines [2] and Rathgeber and Becker [29].

The purpose of this paper is to present results of the scalar concentration field of a sharp-edged rectangular jet injected into a cross stream flow in a square duct. The mean and concentration fluctuation field were measured by marker nephelometry [45]. The bulk of the results are presented in the form of contour maps and transverse profiles of the mean and fluctuation fields at various downstream locations as well as results of the jet spreading rate.

EXPERIMENTAL

A schematic diagram of the flow system used in this work is shown in Fig. 2. The transverse duct flow originated from a wind tunnel that had a 0.836 m^2 (square) cross-section. At the exit of the wind tunnel the cross section was reduced to a square working section, 228.6 mm, on each side with Plexiglas walls. This area reduction provided a contraction ratio of 16:1 with a turbulence intensity of less than 0.1% in the cross stream flow. The wind tunnel working section had a 1.37 m length with the rectangular jet located 203 mm from the entrance to the working

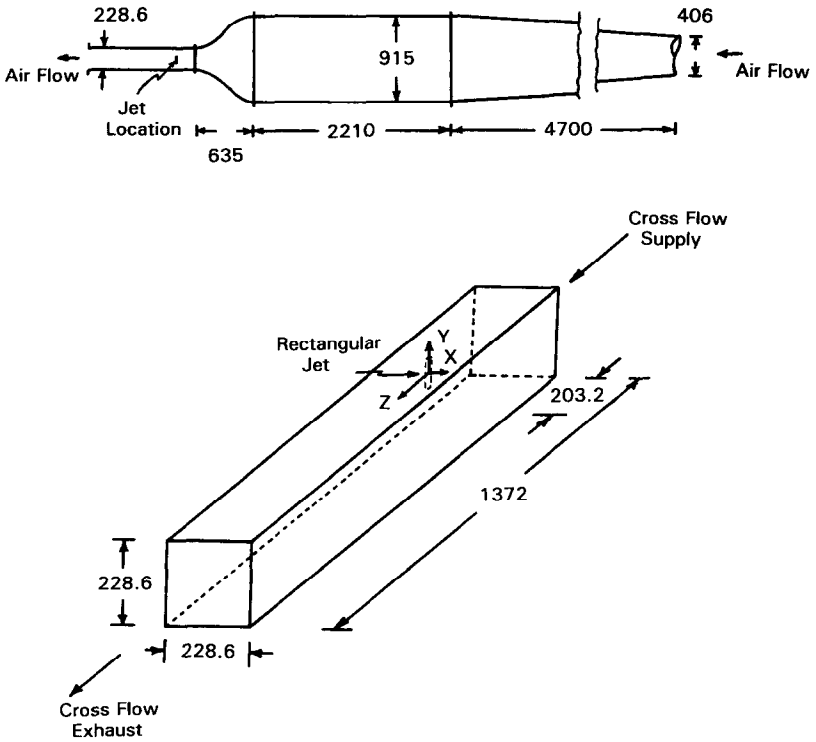

FIG. 2. Schematic diagram of wind tunnel flow system for the cross flow stream (top) and the wind tunnel working section with the cross flow jet (bottom)—dimensions in mm.

section as shown in Fig. 2. The jet was aligned with the jet deflection occurring parallel to the major jet axis—a Cartesian coordinate system is used in conjunction with an orthogonal coordinate axis as shown in Fig. 1. The exit from the test section was connected to an exhaust system for the wind tunnel flow/oil condensation smoke to avoid disturbances in the upstream duct flow near the data acquisition region.

The jet employed in the present work was a sharp-edged orifice cut from thin aluminum plate and mounted in the wall of the Plexiglas test section; care was taken to ensure a flush fit between the plate and the inside wall of the wind tunnel. The cross section of the jet nozzle is shown in Fig. 3. The orifice was sharp-edged with rounded corners, its length, $L_j = 63.5$ mm and width, $D_j = 6.35$ mm with the jet mounted in the vertical position (the long dimension of the jet) relative to the jet flow. Pollard and Iwaniw [46] have shown that the rectangular jet with square and rounded corners has similar characteristics including the presence of a saddle-back behaviour as noted above. The air supply for the jet flow was provided by a compressed air supply used in conjunction with the smoke generator system. The upstream cross section of the jet nozzle was tapered from a 12.7 mm air supply to a 63.5×94.9 mm rectangular section at the nozzle exit. Steel wool was used as an upstream flow distributor to produce a uniform exit velocity profile. A Pitot probe traverse at the jet exit confirmed the presence of a saddle-back behaviour similar to that observed by Quinn *et al.* [39, 40] and Pollard and Iwaniw [46]. Details of the marker nephelometry method are discussed in previous work [41, 45, 47] and the application of it to the present problem is described by Humber [48].

The experimental flow conditions employed in the present work were:

(i) $R = 2.0$; $U_j = 8.4$ m s^{-1} and $U_0 = 4.1$ m s^{-1}

(ii) $R = 3.4$; $U_j = 8.4$ m s^{-1} and $U_0 = 2.5$ m s^{-1}.

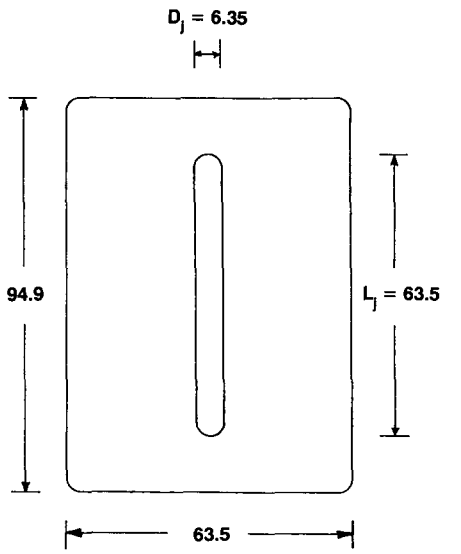

FIG. 3. The rectangular jet nozzle face—dimensions in mm.

The jet velocity corresponds to a Reynolds number of 34 000 based on the long dimension of the nozzle, 3400 based on the narrow dimension and 11 400 based on the hydraulic diameter of a round jet with the same area. The Reynolds numbers for the cross stream flow based on the dimension of the duct working section were 59 700 for $R = 2.0$ and 36 400 for $R = 3.4$.

The primary measurements of interest in this work were the mean and fluctuation signals for the concentration field. Six locations downstream of the jet orifice were used as primary measurement points with cross stream measurements taken at approximately 200–300 points in the plane transverse to the jet axis to provide a grid of data points from which contour plots could be generated. The jet trajectory was chosen to correspond with the maximum concentration, $\bar{\Gamma}_{max}$, along the X-axis, the plane of bilateral symmetry and half concentration points were obtained from the mean concentration data in the transverse planes.

RESULTS

Contour plots of the mean and fluctuation concentration field for $R = 2.0$ and 3.4 are shown in Figs. 4 and 5, respectively, for three downstream locations for each velocity ratio. These results are intended to show the concentration and fluctuation field (i) in the near field, (ii) in an intermediate region where there is deformation of the mean concentration contour field into a kidney shape and (iii) in a region farther downstream where the concentration contours have evolved to a more circular shape. After exiting the nozzle, the jet source fluid concentration field exhibits a horseshoe or kidney shape similar to, but not as extreme as, that noted by Rathgeber and Becker [29]. In particular, a distinct bifurcation of the jet flow is not indicated for the present flow system (as observed with $R > 4$ for round jets in a cross flow [5, 29]). It can also be noted that this kidney shape occurs at lower values of Z/D_j for the higher velocity ratio, $R = 3.4$, as shown in Fig. 5. Farther downstream, near $Z/D_j = 20$, the contours become symmetrical in both cross stream axes. In general, the concentration fluctuation intensity in the core region of the jet was small and this is probably attributable to a lower rate of entrainment for this type of flow. It should be noted that the present work did not extend beyond $Z/D_j = 20$, corresponding to a region of $6D_e$.

From the mean concentration contours, plots of the trajectory of the maximum concentration in the plane of bilateral symmetry were obtained. The trajectory of points estimated in the X–Z plane, Fig. 6, can be described by a power law of the form

$$X/RD_j = 1.91(Z/RD_j)^{0.342}. \quad (2)$$

This correlation agrees reasonably well with the correlation of Pratte and Baines [2] for a round jet in a cross flow but with less deflection near the nozzle and more deflection farther downstream. These data also show less deflection than the rectangular jet with aspect ratio of 4 and $R = 4$ reported by Weston and Thames [43] (for velocity field data)—the data shown by the open squares in Fig. 6 are described by a power law of the form:

$$X/RD_e = 1.19(Z/RD_e)^{0.266}. \quad (3)$$

The mean concentration trajectory data of Rathgeber and Becker [29] at small values of jet to pipe diameter were described by the relation, $X/RD_j = 1.93(Z/RD_j)^{0.20}$, showing close agreement with the present results near $Z/RD_j \approx 1$ but less jet penetration farther downstream. Close examination of Fig. 6 reveals that the power-law fit to the data is marginal, especially for $1 < Z/RD_j < 10$. It is also apparent

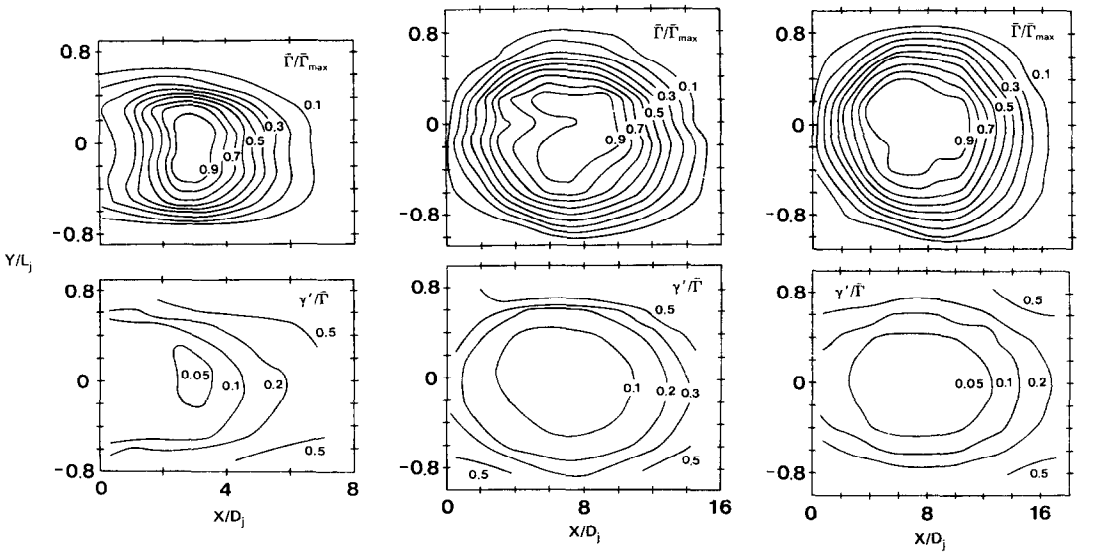

FIG. 4. Contour plots of the mean and concentration fluctuation intensity field for $R = 2$: $Z/D_j = 2$ (left), $Z/D_j = 12$ (middle) and $Z/D_j = 20$ (right).

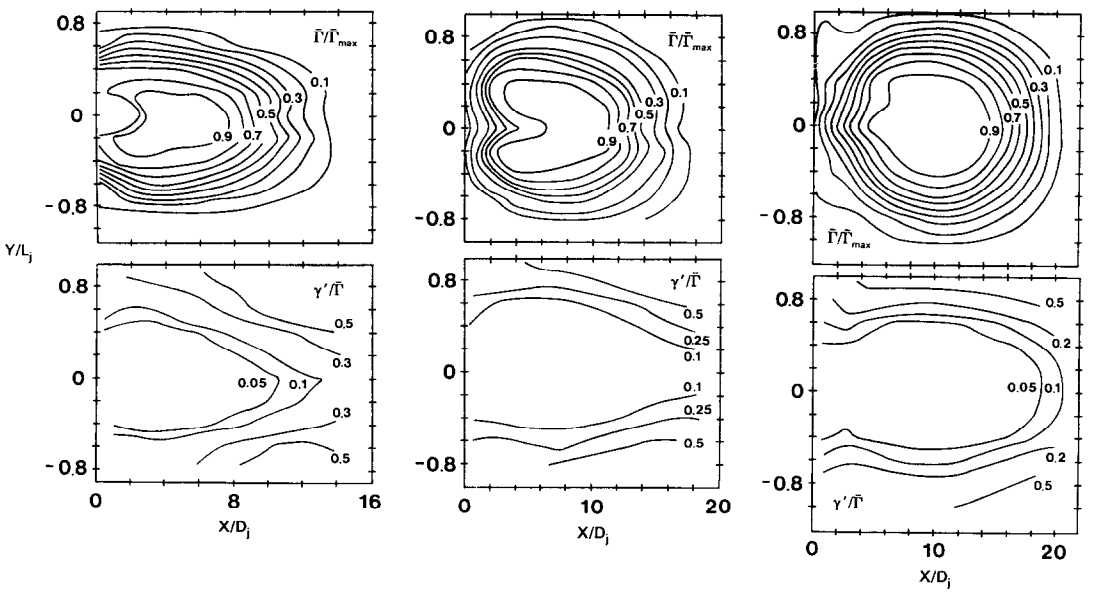

FIG. 5. Contour plots of the mean and concentration fluctuation intensity field for $R = 3.4$: $Z/D_j = 2$ (left), $Z/D_j = 6$ (middle) and $Z/D_j = 12$ (right).

from the general flow structure depicted in Figs. 4 and 5 that the mean concentration contours evolve to a circular cross section sooner for the case with $R = 3.4$—this change occurred beyond $Z/D_j = 12$ for $R = 2$ and $Z/D_j = 6$ for $R = 3.4$. This also corresponds to points in Fig. 6 where, for $1 \leqslant Z/RD_j \leqslant 20$, X/RD_j remains about constant for each velocity ratio. However, if the jet penetration is expressed in terms of the jet trajectory, ξ, as shown in Fig. 7 (similar in form to that used by Pratte and Baines [2]), these two regions are more apparent. In this graph, the jet penetration follows a single relation for the initial region for each velocity ratio where $X/RD_j \propto \xi/RD_j$; however, as each jet approaches a circular cross section the tendency at each R is to follow a power law relation, where $X/RD_j \approx$ constant as ξ/RD_j increases. These data are described by the relations:

$$\xi/RD_j \leqslant 3.3: \quad X/RD_j = (\xi/RD_j)^{0.815} \tag{4}$$

$$R = 2, \xi/RD_j \geqslant 3.3: \quad X/RD_j = 2.21(\xi/RD_j)^{0.167} \tag{5}$$

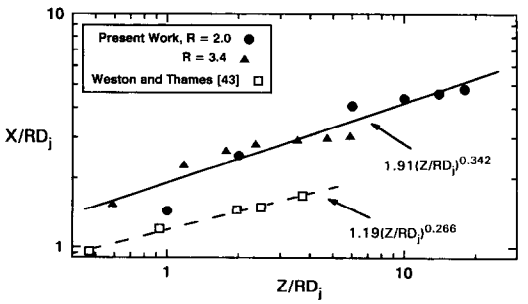

FIG. 6. Jet trajectory expressed in terms of Cartesian coordinates.

$$R = 3.4, \xi/RD_j \geqslant 5: \quad X/RD_j = 2.90(\xi/RD_j)^{0.169}. \tag{6}$$

Keffer and Baines [1] and Pratte and Baines [2] observed that $X/RD_j \approx \xi/RD_j$ for low values of ξ over a wide range of jet penetration values, $0.1 \leqslant$

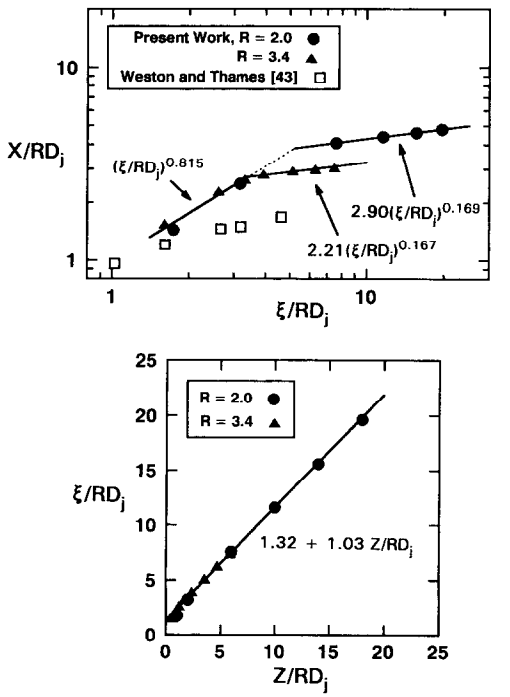

FIG. 7. Jet penetration as a function of trajectory path (top graph) and jet trajectory as a function of Cartesian coordinate position in the downstream direction (bottom graph).

$\xi/RD_j \leqslant 1$. Following this initial high penetration rate Pratte and Baines observed a gradual transition ($1 \leqslant \xi/RD_j \leqslant 3$) to a lower penetration rate described by a 1/3 power law for $\xi/RD_j > 3$. In the present work, accurate estimates of the jet trajectory could not be made below $\xi/RD_j = 1.5$, but the present results, equation (4), do not differ significantly from these observations and it is interesting to note that the power law exponents in equations (5) and (6) are nearly equal for each velocity ratio. The data of Weston and Thames [43] shown in the top graph of Fig. 7 are limited to the region $\xi/RD_j < 4$ but their results do appear to tend to be of the form of equation (4) for $\xi/RD_j < 1.0$ and a power law form similar to equations (5) and (6) farther downstream.

The jet trajectory can also be described by the relation, Fig. 7 (bottom graph),

$$\xi/RD_j = 1.32 + 1.03Z/RD_j \tag{7}$$

in close agreement with the result of Rathgeber and Becker [29], $\xi/RD_j = 1 + Z/RD_j$, for the trajectory of a round jet into a pipe flow.

The concentration half width, defined as that point in the Y- or X-plane where $\bar{\Gamma}/\bar{\Gamma}_{max} = 0.5$, provides a measure of the spreading rate of the jet as it proceeds downstream. These results, Fig. 8, exhibit good symmetry in the Y-plane (plane of bilateral symmetry); however, results for the X-plane differ on each side of the jet trajectory and these values are denoted by $+b_x$ and $-b_x$ for the upstream and downstream sides of the jet respectively. Those data for the Y-direction are shown in the top graph of Fig. 8 and are described by linear relations,

$$R = 2: \quad b_y/RD_j = 2.28 + 0.109\xi/RD_j \tag{8}$$

$$R = 3.4: \quad b_y/RD_j = 1.34 + 0.159\xi/RD_j. \tag{9}$$

The data in the X-direction are shown in the two middle graphs of Fig. 8 and are described by power law relations,

$$-b_x/RD_j = 0.871(\xi/RD_j)^{0.572} \tag{10}$$

$$+b_x/RD_j = 0.925(\xi/RD_j)^{0.458}. \tag{11}$$

Rathgeber and Becker [29] also observed a power law behaviour and a similar degree of scatter for the half concentration width in the plane of bilateral symmetry for the round jet in a cross flow (they did not report measurements comparable to the b_x data noted above). The present results for $R = 2$ indicate that the half concentration width is comparable in both planes while the results for $R = 3.4$ indicate a higher spreading rate on the leading edge of the jet than on the trailing edge in the plane of bilateral symmetry. Farther downstream, the half concentration widths for flow conditions appear to tend to similar values in both planes. Data from the contour plots can also be used to estimate an equivalent half concentration radius of the form,

$$b_{1/2} = (A_{1/2}/\pi)^{1/2} \tag{12}$$

where $A_{1/2}$ is the area described by the contour $\bar{\Gamma}/\bar{\Gamma}_{max} = 0.5$ (this length scale was first proposed by Kamotani and Greber [5] for analysis of jets in a cross flow). The data for this half concentration radius are described by a linear relation, Fig. 8 (bottom graph),

$$b_{1/2}/RD_j = 1.41 + 0.162\xi/RD_j. \tag{13}$$

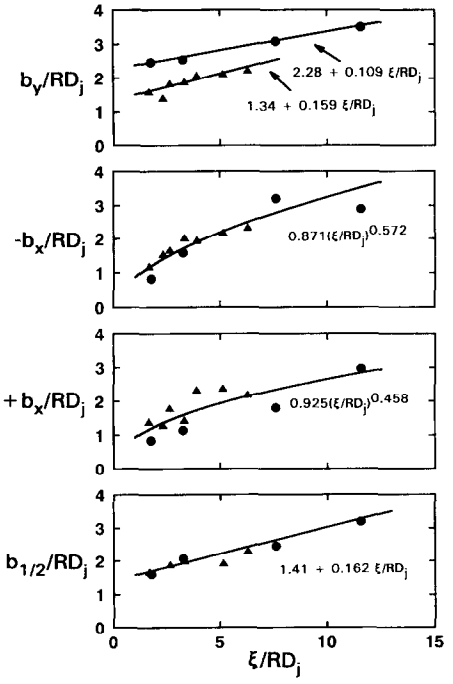

FIG. 8. Jet half concentration lengths as a function of distance along the jet trajectory; from top to bottom, graphs display b_y, $-b_x$, $+b_x$ and $b_{1/2}$: $R = 2.0$ (circles) and $R = 3.4$ (triangles).

The transverse profiles of the mean concentration are shown in Fig. 9 where the transverse position is normalized with respect to the appropriate half concentration width. These results exhibit good symmetry within the experimental error expected for these measurements and the data are presented with the data 'folded over' along the jet trajectory. The Gaussian type distribution observed in free jets (e.g. Becker *et al.* [49]) is also shown in these graphs.

Transverse profiles of the concentration fluctuation intensity are shown in Fig. 10 for both transverse planes and velocity ratios. Data for the plane of bilateral symmetry are depicted with an 'open' and 'closed' symbol for results on opposite sides of the jet trajectory. Within the experimental error expected for these measurements, the results for the Y-plane exhibit good symmetry and a steep gradient in the fluctuation intensity for $Y/b_y > 1$. The results for the X-plane are not necessarily symmetrical and these data are shown with an 'open' symbol to denote the upstream side of the jet and a 'closed' symbol to denote results for the leeward side of the jet. The greatest difference in these results occurred for $R = 2$ in the near field, typically $Z/RD_j = 1$ and 2, where the results for the upstream

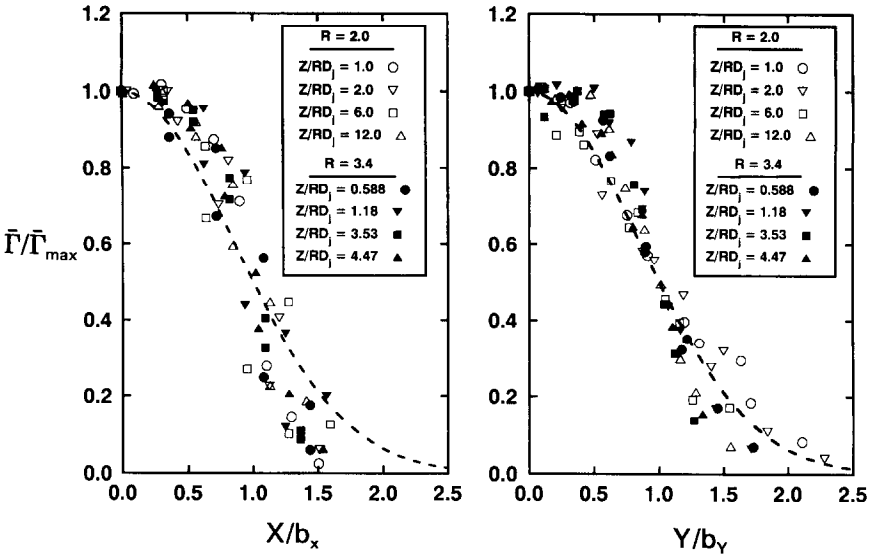

FIG. 9. Transverse profiles of the mean concentration from the maximum value ($\bar{\Gamma}_{max}$) along the jet trajectory. Dashed line represents a Gaussian type distribution, exp $\{-0.693(X/b_x)^2\}$ or exp $\{-0.693(Y/b_y)^2\}$.

side of the jet were higher. These results in Fig. 10 generally exhibit the expected behaviour with low values of $\gamma'/\bar{\Gamma}$ in the core region rising to higher values near the edge of the jet in both planes. Higher fluctuation intensities were observed in the Y-plane for each flow condition and these data also exhibited a higher gradient in the cross stream values of $\gamma'/\bar{\Gamma}$ than the X-plane or those of a round jet [49]. The action of the cross stream fluid thus causes a rapid mixing towards the edge of the jet in the plane of bilateral symmetry. However in the core of the jet there is less mixing as indicated by the lower fluctuation intensities for the X-plane and for $Y/b_y < 1$ in the Y-plane.

DISCUSSION OF RESULTS

The contours of the mean and fluctuation concentration fields, Figs. 4 and 5, provide a clear picture of the development of this type of flow system. At $Z/D_j = 2.0$, a kidney shaped profile is clearly evident

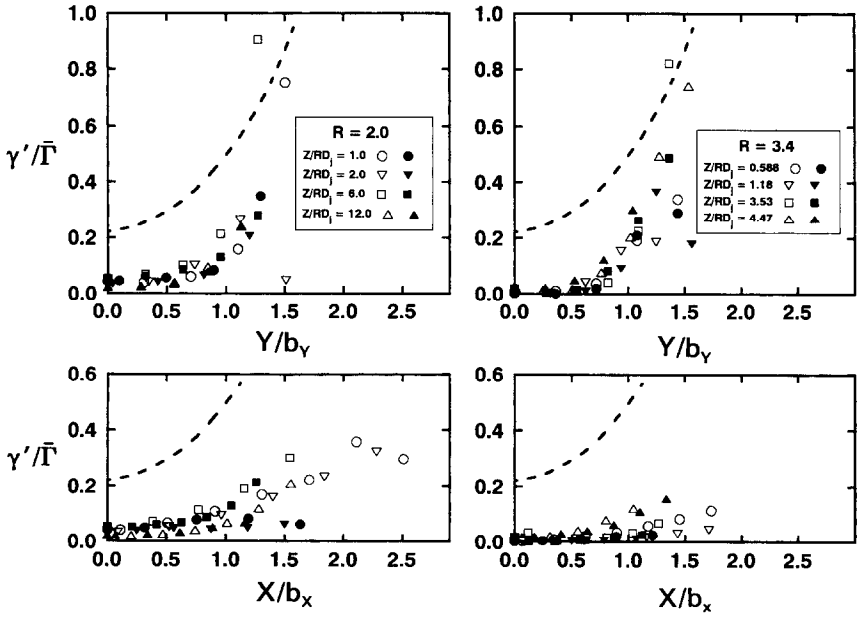

FIG. 10. Transverse profiles of the concentration fluctuation intensity. 'Open' and 'closed' symbols represent data on opposite sides of the jet trajectory for the Y-plane and the upstream and leeward side of the jet for the X-plane. Dashed line represents the free turbulent jet in quiescent surroundings [49].

for $R = 3.4$ and to a lesser extent for $R = 2.0$. The greater penetration of the jet for $R = 3.4$ is also evident at this downstream location. At the next downstream location shown in Figs. 4 and 5 ($Z/D_j = 12$ for $R = 2.0$ and $Z/D_j = 6.0$ for $R = 3.4$), both jets have developed into a kidney shaped contour (typically the maximum jet deformation observed for each flow condition). At this point, the mean concentration mappings are quite similar indicating that the jet deformation occurs faster for $R = 3.4$. These mean concentration contours are also similar to the cross sectional shape observed by Rathgeber and Becker [29] and Pollard [50]. At the last downstream contour profile for each flow condition, the jet cross section approaches a circular form where the width of the jet in the Y- and Z-planes are almost equal in magnitude. In this region, the rectangular cross flow jet differs from the round jet which forms and maintains a distinct bifurcated structure [29]. It is also apparent that the cross flow has a significant effect on this flow development as the jet with $R = 3.4$ (greater penetration into the cross flow) tended to a circular cross section faster than the jet with $R = 2.0$. It is also likely that the development of the jet with $R = 2$ is affected by the closer proximity of the wall boundary—Keffer and Baines [1] first noted a wall hindrance effect on jet entrainment for $R = 2$ in a round jet in a cross flow.

It should be noted that the jet trajectory data described by equation (2), Fig. 6, exhibit scatter similar to previous measurements of this parameter for round jets in a cross flow. However, there is also a trend in the residuals for each flow condition, with lower trajectory values predicted at intermediate values of Z/RD_j. It is interesting to note that this region also corresponds to the point where the maximum jet deformation takes place ($Z/D_j \approx 12$ for $R = 2$ and $Z/D_j \approx 6$ for $R = 3.4$) suggesting that a change in trajectory path occurs as the jet changes from an initial rectangular shape to the circular cross section observed farther downstream. This effect is confirmed by the correlation shown in Fig. 7 with the jet trajectory expressed in X–ξ coordinates. In the initial region, $\xi/RD_j \leqslant 3$, both jets appear to follow a similar path corresponding to the zone of maximum jet deflection noted by Keffer and Baines [1] and Pratte and Baines [2]. In these previous studies a linear relation, $X/RD_j \approx \xi/RD_j$, was observed for $\xi/RD_j \leqslant 1.5$ followed by a transition region to a power law region (the vortex zone noted by Pratte and Baines [2]), $X/RD_j \propto (\xi/RD_j)^{1/3}$, farther downstream, $\xi/RD_j \geqslant 3$. The present data for $\xi/RD_j \leqslant 3$ appear to follow a transition behaviour similar to that observed by Pratte and Baines [2] but more data would be required at lower values of ξ to confirm the linear form noted above. It can be also noted that the shape of the rectangular jet in the cross flow undergoes some changes in the nozzle region (the case for $R = 3.4$, Fig. 5, best demonstrates this behaviour). Farther downstream the present results also tend to power law forms where $\xi/RD_j \propto (X/RD_j)^n$ with $n \approx 0.17$ for each flow rate. The start of this region occurs at $\xi/RD_j \approx 5$ for $R = 2$ and $\xi/RD_j \approx 3$ for $R = 3.4$ and corresponds to the point where there is a large distortion in the jets, leading to a more circular cross section farther downstream. The displacement of these power law regions for each jet velocity corresponds to a different effective source for the new jet shape as the flow progresses in the downstream direction.

The low fluctuation intensity values observed in the core region for the rectangular cross flow jet, Figs. 4 and 5, is significantly different from the round jet case where the bifurcated flow leads to very high fluctuation intensities, typically $\gamma'/\bar{\Gamma} \approx 0.4$, along the jet trajectory [29]. The cross flow fluid does not produce this high level of fluctuation intensity in a rectangular jet with an aspect ratio of 10 for $R \leqslant 3.4$.

The concentration half width provides a good parameter with which to measure the spreading rate of jets. In the Y-plane, the concentration half width should be equal on both sides of the jet since this plane defines the plane of bilateral symmetry. In the X-plane, the concentration half width for a round jet in a cross flow is typically shorter during early stages of the flow development on the leading edge than on the trailing or downstream edge [29]. While this behaviour is suggested by the correlations presented in equations (10) and (11) and the results shown in Fig. 8 (two centre graphs), the effect is not large and within the scatter of the present data, the half concentration width in both planes appears to be nearly equal farther downstream, near $Z/RD_j \approx 10$. The half concentration width expressed in terms of the effective radius of the 50% mean concentration contour, $b_{1/2}$, exhibit a good linear relation for both flow conditions. The jet spreading rate, $b_{1/2} \approx 0.162\ \xi$, given by equation (13) is comparable to the spreading rate in the free rectangular jet with the same aspect ratio, where $b_z \approx 0.130\ \xi$ and $b_y \approx 0.152\ \xi$ [41], and significantly greater than a free round jet where $b_{1/2} \approx 0.106\ \xi$ [49].

The transverse profiles of the mean concentration, Fig. 9, indicate a certain amount of scatter in these data but no distinctive pattern is obvious except that the X-plane data appear to approach a Gaussian type distribution faster than the Y-plane data for both flow conditions. Kamotani and Greber [5] and Rathgeber and Becker [29] also observed a Gaussian type behaviour for the plane of bilateral symmetry for a round jet in a cross flow, particularly for $1 \leqslant \bar{\Gamma}/\bar{\Gamma}_{max} \leqslant 0.5$. It is also worth noting that, within the accuracy of the mean concentration measurements, there is no evidence of the saddle-back behaviour observed in the free rectangular jet emanating from a sharp edged nozzle [41].

Transverse profiles of the concentration fluctuation intensity in the present work show good symmetry for the Y-plane while the data for the Z-plane exhibit some asymmetry in the near field for the case of $R = 2.0$ where there appears to be higher values on the

leading edge of the jet. Rathgeber and Becker [29] also observed higher values of the fluctuation intensity on the upstream side of a round jet in a cross flow. The low values of $\gamma'/\bar{\Gamma}$ in the core region of the jet indicate a lower level of mixing than is encountered for a round jet in a cross flow. This is consistent with the general shape of the concentration contour diagrams that do not indicate a bifurcated flow pattern; however, there does appear to be intense mixing on the outer edge of the jet, $Y \geqslant b_y$ in the Y-plane. In this region, there is a sharp increase in the fluctuation intensity due to the interaction with the cross stream flow. The transverse gradient in the $\gamma'/\bar{\Gamma}$ profiles in the Y-plane for $Y/b_y > 1.0$ appear to be higher than those of a free round jet in quiescent surroundings [49]. This rapid mixing and the distortion of the jet in the Y-plane due to the cross flow stream also appears to counter the persistence of the saddle-back behaviour of the mean concentration profiles at a much earlier stage than observed in the free rectangular jet. This saddle-back phenomena has been observed in the near field region ($X/D_e \leqslant 10$) of jets issuing from a sharp-edged orifice near $Y/b_y \approx 0.6$–0.8 [39–41] and a wall jet flow issuing from a sharp edged rectangular orifice [42]. The near field contour plots shown in Figs. 4 and 5 do not indicate such behaviour for the rectangular jet in a cross flow near $Z/D_j = 2$. The transverse mean concentration data, Fig. 9, exhibit a mean concentration decay, $\bar{\Gamma}/\bar{\Gamma}_{max} \approx 0.8$–$0.85$, in the near field near $Y/b_y = 0.6$–0.8.

The data presented in this paper represents an intermediate range of the velocity ratio, R. Krothapalli *et al.* [44] found that the normalized upstream separation distance increased in the range $R \leqslant 5$ and decreased for higher velocity ratios. They attributed the increase at lower R values to a weaker entrainment on the leeward side of the jet and the present results appear to confirm this hypothesis. The mean and fluctuation field contour diagrams, Figs. 4 and 5, show that the leeward side of the nozzle fluid field extends to the wall region ($X = 0$) and that there is a lower level of mixing in the core region of the jet compared to the more intense mixing observed in the round jet in a cross flow stream at larger values of R. Kamotani and Greber [5] have noted that the scalar field exhibited a peak mean value off the plane of bilateral symmetry for $R \approx 8$, but the peak value remained on the bilateral symmetry plane for $R \leqslant 4$ in the round jet cross flow system. This phenomenon was attributed to more rapid mixing as the jet is able to more readily entrain cross stream fluid with less wall boundary interference at larger velocity ratios. It thus appears that such a phenomenon may indeed occur with rectangular jets but with a slightly higher critical velocity ratio, $R \approx 5$.

CONCLUSION

The scalar concentration field of a sharp-edged rectangular jet with an aspect ratio of 10 mixing with a cross stream flow has been examined using marker nephelometry. Measurements include the fields of the mean and fluctuation concentration fields for $\xi/RD_j \leqslant 6$ for $R = 3.4$ and $\xi/RD_j \leqslant 20$ for $R = 2.0$. The principal findings of this work are:

(1) The jet trajectory follows an initial high penetration region similar to that of a round jet followed by a region further downstream where the jet path is proportional to $(\xi/RD_j)^{0.17}$.

(2) The half concentration length in the Y- and X-planes follow linear and power law forms respectively as a function of the distance along the jet trajectory. The half concentration length based on the effective radius of the $\bar{\Gamma}/\Gamma_{max} = 0.5$ contour follows a linear relation with a spreading rate that is slightly larger than the free rectangular jet.

(3) Transverse profiles of the mean concentration field in the plane of bilateral symmetry were closer to a Gaussian type behaviour than those data in the Y-plane. The fluctuation intensity data were significantly lower in the plane of bilateral symmetry than in the Y-plane.

(4) The jets exhibited a kidney shape similar to a round jet in a cross flow but the rectangular jet did not exhibit a bifurcated structure for $R = 2.0$ and 3.4. In the core region of the jets there was a relatively low fluctuation intensity indicating a lower mixing intensity than round jets in a cross flow at larger values of the velocity ratio.

(5) The sharp-edged rectangular jet in a cross flow did not exhibit a saddle-back behaviour in the mean concentration field in the near field region ($Z/D_j = 2$). The action of the cross flow stream thus appears to counter the mechanism for the persistence of this phenomena more quickly than the free rectangular jet.

Acknowledgements—This work was supported by grants from the Natural Sciences and Engineering Research Council of Canada. One of the authors (EWG) wishes to acknowledge excellent sabbatical leave facilities provided by the Australian Pulp and Paper Institute (Monash University, Clayton, Vic.) and the Department of Chemical and Materials Engineering, University of Auckland (Auckland, New Zealand) during the preparation of this paper.

REFERENCES

1. J. F. Keffer and W. D. Baines, The round jet in a cross-wind, *J. Fluid Mech.* **15**, 481–496 (1963).
2. B. D. Pratte and W. D. Baines, Profiles of the round jet in a cross flow, *J. Proc. Amer. Soc. Civil Engng* **93**, HY-6, 53–64 (1967).
3. M. A. Patrick, Experimental investigation of the mixing and penetration of a round turbulent jet injected perpendicularly into a transverse stream, *Trans. Inst. Chem. Engrs* **45**, T16–T31 (1967).
4. H. M. McMahon, D. D. Hester and J. G. Palfrey, Vortex shedding from a turbulent jet in a cross-wind, *J. Fluid Mech.* **48**, 73–80 (1971).
5. Y. Kamotani and I. Greber, Experiments on a turbulent jet in a cross flow, *AIAA J.* **10**, 1425–1429 (1972).
6. R. L. Stoy and Y. Ben-Haim, Turbulent jets in a confined crossflow, *ASME J. Fluids Engng* **95**, 551–556 (1973).

7. P. Chassaing, J. George, A. Claria and F. Sananes, Physical characteristics of subsonic jets in a cross-stream, *J. Fluid Mech.* **62,** 41–64 (1974).
8. J. Sucec and W. W. Bowley, Prediction of the trajectory of a turbulent jet injected into a crossflowing stream, *ASME J. Fluids Engng* **98,** 667–673 (1976).
9. T. Makihata and Y. Miyai, Trajectories of single and double jets injected into a crossflow of arbitrary velocity distribution, *J. Fluids Engng* **101,** 217–223 (1979).
10. D. Crabb, D. F. G. Durao and J. H. Whitelaw, A round jet normal to a cross-flow, *J. Fluids Engng* **103,** 142–153 (1981).
11. J. Andreopoulos, Measurements in a jet-pipe flow issuing perpendicularly into a cross-stream, *J. Fluids Engng* **104,** 493–499 (1982).
12. J. Andreopoulos and W. Rodi, An experimental investigation of jets in a crossflow, *J. Fluid Mech.* **138,** 93–127 (1984).
13. R. Fearn and R. P. Weston, Vorticity associated with a jet in a cross flow, *AIAA J.* **12,** 1666–1671 (1974).
14. Z. M. Moussa, J. W. Trischka and S. Eskinazi, The near field in the mixing of a round jet with a cross-stream, *J. Fluid Mech.* **80,** 49–80 (1977).
15. D. Crabb, D. F. G. Durao and J. H. Whitelaw, A round jet normal to a crossflow, *ASME J. Fluids Engng* **103,** 142–153 (1981).
16. J. Andreopoulos, Measurements in a jet-pipe flow issuing perpendicularly into a cross stream, *ASME J. Fluids Engng* **104,** 493–499 (1982).
17. J. E. Broadwell and R. E. Breidenthal, Structure and mixing of a transverse jet in incompressible flow, *J. Fluid Mech.* **148,** 405–412 (1984).
18. J. Andreopoulos, On the structure of jets in a crossflow, *J. Fluid Mech.* **157,** 163–197 (1985).
19. R. H. Nunn, Vorticity growth and decay in the jet in a cross flow, *AIAA J.* **23,** 473–475 (1985).
20. P. R. Sterland and M. A. Hollingsworth, Experimental study of multiple jets directed to a cross-flow, *J. Mech. Engng Sci.* **17,** 117–124 (1975).
21. Z. A. Khan and J. H. Whitelaw, Mean velocity and concentration characteristics downstream of rows of jets in a cross-flow, *J. Heat Transfer* **102,** 391–392 (1980).
22. L. S. Cohen, L. J. Coulter and W. J. Egan, Penetration and mixing of multiple gas jets subjected to a cross flow, *AIAA J.* **9,** 718–724 (1971).
23. H. Ziegler and P. T. Wooler, Multiple jets exhausting into a crossflow, *J. Aircraft* **8,** 414–420 (1971).
24. J. D. Holdeman and R. E. Walker, Mixing of a row of jets with a confined cross flow, *AIAA J.* **15,** 243–249 (1977).
25. K. M. Isaac and J. A. Schetz, Analysis of multiple jets in a cross flow, *J. Fluids Engng* **104,** 489–492 (1982).
26. T. Makihata and Y. Miyai, Prediction of the trajectory of triple jets in a uniform crossflow, *J. Fluids Engng* **105,** 91–97 (1983).
27. K. M. Isaac and A. K. Jakubowski, Experimental study of the interaction of multiple jets with a cross flow, *AIAA J.* **23,** 1679–1683 (1985).
28. J. W. Ramsey and R. J. Goldstein, An interaction of a heated jet with a deflecting stream, *J. Heat Transfer* **94,** 365–372 (1971).
29. D. E. Rathgeber and H. A. Becker, Mixing between a round jet and a transverse turbulent pipe flow, *Can. J. Chem. Engng* **61,** 148–157 (1983).
30. J. Andreopoulos, Heat transfer measurements in a heated jet-pipe flow issuing perpendicularly into a cold stream, *Phys. Fluids* **26,** 3201–3210 (1983).
31. D. Adler and A. Baron, Prediction of a three-dimensional circular turbulent jet in a crossflow, *AIAA J.* **17,** 168–174 (1979).
32. M. L. Bojic and S. Eskinazi, Two-dimensional model of a nonbuoyant jet in a crossflow, *AIAA J.* **17,** 1050–1054 (1979).
33. S. L. V. Coelho and J. C. R. Hunt, The dynamics of the near field of strong jets in crossflows, *J. Fluid Mech.* **200,** 95–120 (1989).
34. J. C. Chien and J. A. Schetz, Numerical solution of the three dimensional Navier–Stokes equations with applications to channel flows and a buoyant jet in a cross flow, *ASME J. Appl. Mech.* **42,** 575–579 (1975).
35. S. V. Patankar, D. K. Basu and S. A. Alpay, Predictions of the three dimensional velocity field of a deflected turbulent jet, *ASME J. Fluids Engng* **99,** 758–762 (1977).
36. A. O. Demuren, Numerical calculations of steady three dimensional turbulent jets in cross flow, *Comp. Meth. Appl. Mech. Engng* **37,** 309–328 (1983).
37. A. O. Demuren and W. Rodi, Three-dimensional numerical calculations of flow and plume spreading past cooling towers, *J. Heat Transfer* **109,** 113–119 (1987).
38. M. Fairweather, W. P. Jones and A. J. Marquis, Predictions of the concentration field of a turbulent jet in a cross flow, *Combust. Sci. Technol.* **62,** 61–76 (1988).
39. W. R. Quinn, A. Pollard and G. F. Marsters, Measurements in a turbulent rectangular free jet, *4th Symp. on Turbulent Shear Flows*, pp. 7.1–7.6 (1983).
40. W. R. Quinn, A. Pollard and G. F. Marsters, Mean velocity and static pressure distribution in a three dimensional free jet, *AIAA J.* **23,** 971–973 (1985).
41. E. W. Grandmaison, A. Pollard and S. Ng, Scalar mixing in a free, turbulent rectangular jet, *Int. J. Heat Mass Transfer* **34,** 2653–2662 (1991).
42. A. Pollard and R. R. Schwab, The rectangular wall jet, *Experiments in Fluids* (submitted) (1993).
43. R. P. Weston and F. C. Thames, Properties of aspect ratio 4 rectangular jets in a subsonic crossflow, *J. Aircraft* **17,** 701–707 (1979).
44. A. Krothapalli, L. Lourenco and J. M. Buchlin, Separated flow upstream of a jet in a crossflow, *AIAA J.* **28,** 414–420 (1990).
45. H. A. Becker, Marker nephelometry, concentration fluctuations and turbulent mixing. In *Studies in Convection*, Vol. 2 (Edited by B. E. Launder), pp. 45–105. Academic Press, London (1977).
46. A. Pollard and M. A. Iwaniw, Flow from sharp-edged rectangular orifices, the effect of corner rounding, *AIAA J.* **23,** 631–633 (1985).
47. E. W. Grandmaison, S. Ng and H. A. Becker, A smoke generation system for fluid dynamics research, *J. Phys. Series E: Scient. Instrum.* **20,** 606–608 (1987).
48. A. Humber, Mixing between a sharp-edged rectangular jet and a transverse channel flow, M.Sc. Thesis, Dept. of Chemical Engineering, Queen's University, Kingston, Ont., Canada K7L 3N6 (1991).
49. H. A. Becker, H. C. Hottel and G. C. Williams, The nozzle fluid concentration field of the round, turbulent, free jet, *J. Fluid Mech.* **30,** 285–303 (1967).
50. A. Pollard, Flow in tee junctions, Ph.D. Thesis, University of London (1978).